X-9

Copy 261
RM E51H28

RESEARCH MEMORANDUM

INVESTIGATION OF AFTERBURNER PERFORMANCE AND AFTERBURNER FUEL SYSTEM COKING OF THE WESTINGHOUSE XJ34-WE-32 ENGINE

By Lewis E. Wallner and William R. Prince

Lewis Flight Propulsion Laboratory
Cleveland, Ohio

NATIONAL ADVISORY COMMITTEE FOR AERONAUTICS

WASHINGTON

February 21, 1952

219.98/13

NATIONAL ADVISORY COMMITTEE FOR AERONAUTICS

RESEARCH MEMORANDUM

INVESTIGATION OF AFTERBURNER PERFORMANCE AND AFTERBURNER FUEL SYSTEM COKING OF THE WESTINGHOUSE XJ34-WE-32 ENGINE

By Lewis E. Wallner and William R. Prince

SUMMARY

An investigation of the performance of the Westinghouse XJ34-WE-32 engine with afterburner operative was made in the altitude wind tunnel at simulated altitudes from 10,000 to 40,000 feet and flight Mach numbers from 0.52 to 1.05. During the course of the performance work, the fuel-injection holes in the afterburner fuel manifold became plugged because of coke or carbon deposits in the manifold. As a result, a later study was made of this coking problem in an attempt to determine its effect on the afterburner performance.

Changes in altitude and flight Mach number had the normal effects on the afterburning performance parameters; that is, increased pressure in the afterburner raised the combustion efficiency and lowered the specific fuel consumption. Peak combustion efficiencies of 95 and 60 percent were obtained at altitudes of 10,000 and 40,000 feet, respectively. However, reproducible afterburner performance is difficult to obtain because of the coke deposits in the injection holes of the afterburner fuel manifold. Losses in thrust up to 8 percent of the total net thrust of the engine were obtained in a number of instances when some of the fuel-manifold injection holes were plugged with coke deposits. It was found that the formation of coking might be eliminated by the complete purging of the afterburner fuel system with air at the same instant the afterburner was shut off.

INTRODUCTION

As part of a comprehensive investigation of the Westinghouse XJ34-WE-32 engine, the performance of the engine with the production afterburner operative was investigated in the NACA Lewis altitude wind tunnel. The XJ34, an experimental engine, consisted of a J34 turbojet engine coupled to an afterburner which has a variable-area exhaust nozzle, a 3-ring variable-flow fuel-injection system, a two-V flame holder, and an internal cooling liner. The engine-afterburner combination was

controlled by means of an automatic electronic control. Several modifications, which are described in the section APPARATUS AND INSTRUMENTATION, were made to the production XJ34-WE-32 afterburner.

Afterburner performance data were obtained over a range of afterburner fuel-air ratio at constant turbine-outlet temperature for altitudes from 10,000 to 40,000 feet and flight Mach numbers from 0.52 to 1.05. The variation of thrust augmentation, specific fuel consumption, afterburner combustion efficiency, and exhaust-gas temperature with afterburner fuel-air ratio is shown. In addition, the effect of altitude and ram pressure ratio on the lean blow-out limits of the afterburner were determined.

During the afterburner performance investigation, difficulty was encountered with "coke" or hard carbon deposits which plugged the fuel-injection holes in the afterburner fuel manifold. This plugging of the fuel manifold resulted in altered fuel distribution, which affected afterburner performance. Adequate time to permit a thorough investigation of the coking problem and its possible solution was unavailable; however, data are presented herein to indicate the effect of the coke deposits on the afterburner performance. These coking results therefore do not represent a comprehensive investigation of the problem but rather give a presentation of the information obtained on the coking characteristics of this particular afterburner geometry during the performance calibration.

APPARATUS AND INSTRUMENTATION

Installation

The engine-afterburner combination was mounted on a wing section that spanned the 20-foot-diameter test section of the altitude wind tunnel (fig. 1).

Engine

The XJ34-WE-32 is an axial-flow turbojet engine consisting of an 11-stage compressor, a double annular combustor, a 2-stage turbine, and an integral afterburner. The engine with afterburner inoperative has a static sea-level rating of 3370 pounds thrust at an engine speed of 12,500 rpm and a maximum allowable turbine-inlet temperature of 1525° F. With afterburner operating at full augmentation and basic engine at rated thrust, the total rated sea-level static thrust is 4900 pounds. At this operating condition, the air flow is approximately 58 pounds per second.

The engine is equipped with an electronic control that, for the afterburning case, varies exhaust-nozzle area to maintain engine operation at a constant turbine-outlet temperature over a range of tail-pipe fuel-air ratio.

Afterburner

A cross-sectional sketch of the engine-afterburner assembly with flame holder and fuel system installed is shown in figure 2. The overall length of the assembly was 184 inches with a maximum afterburner diameter of 27 inches and a total dry weight of 1558 pounds. The afterburner, with a total length of approximately 89 inches (fig. 3), was attached to the turbine-outlet flange and consisted of three basic sections: diffuser, combustion chamber, and exhaust nozzle. The diffuser section, which was 24 inches long, expanded from an annular inlet having an outer diameter of 21 inches to an outlet $25\frac{1}{2}$ inches in diameter and had an outlet- to inlet-area ratio of approximately 2.5. The cylindrical combustion chamber was approximately 30 inches long with an internal diameter of $25\frac{1}{2}$ inches. Fuel was injected in an axial downstream direction at the inlet of the combustion chamber through a three-ring internal manifold having a total of 168 holes averaging 0.030 inch in diameter (fig. 3). A 2-V annular-gutter-type flame holder (area blockage, 35 percent) was mounted about 2 inches downstream of the fuel manifold. An internal cooling liner with approximately 1/2-inch radial space between the liner and the outer shell extended the length of the combustion chamber. The nozzle consisted of a converging section with a half-cone-angle of approximately 10° and a length of approximately 35 inches. A variable-area clam-shell-type nozzle was attached to the end of the converging section of the afterburner. The area variation available with this nozzle was between 160 and 300 square inches.

The following modifications were made to the production afterburner to facilitate testing in the altitude wind tunnel: (1) the afterburner segment of the electronic control was disconnected; (2) the ejector cooling shroud was removed; and (3) the variable-flow 3-ring fuel-injection system was modified so that fuel was injected at constant pressure through all three rings simultaneously. It is believed that these modifications did not materially affect the performance calibration of the production burner for the range of afterburner fuel flows investigated.

Instrumentation

Temperature and pressure measurements were obtained at several stations in the engine and the afterburner as shown in figure 2. Engine

air flow (station 1) was calculated from measurements with survey rakes mounted in the inlet-air duct attached to the inlet of the engine. A complete pressure and temperature survey was obtained at the turbine outlet (station 5), and total and static pressures at the exhaust-nozzle outlet (station 8) were measured with a water-cooled survey rake. In order to obtain a correction to the scale thrust measurements, the drag of the water-cooled rake was determined by means of an air-balance piston mechanism. All fuel flows were measured by calibrated rotameters.

The engine electronic control had a separate indication of the turbine-outlet temperature by means of nine parallel thermocouple probes, which were immersed into the gas stream 3/4 of the annular passage height, $17\frac{3}{8}$ inches downstream of the turbine.

Procedure

The afterburner was operated over a range of afterburner fuel flow at a flight Mach number of 0.52 for altitudes from 10,000 to 40,000 feet, and at flight Mach numbers from 0.52 to 1.05 at an altitude of 40,000 feet. At each flight condition, with the engine operating at rated speed and maximum turbine-outlet temperature, the afterburner fuel flow was varied from a minimum determined by lean blow-out to a maximum determined by a limitation of the exhaust-nozzle size.

Engine-inlet air pressures corresponding to altitude flight conditions were obtained by introducing dry refrigerated air from the tunnel make-up air system through a duct to the engine inlet. This duct was connected to the engine inlet by means of a slip joint with a frictionless seal so that the thrust and drag could be measured by the balance scales. Air was supplied to the engine at NACA standard conditions, except that the minimum temperature obtained was about 0° F. The air was throttled from approximately sea-level pressure to the desired total pressure at the engine inlet. Complete free-stream ram pressure recovery was assumed at each flight condition in the calculation of flight Mach number.

Thrust measurements were obtained from the balance scales and from a pressure survey at the exhaust-nozzle outlet. The thrust values presented herein were obtained from the balance-scale measurements. The definition of net-thrust augmentation ratio is given in appendix A. Exhaust-gas temperatures were based on thrust measurements from the balance scales and pressure measurements at the exhaust-nozzle outlet.

Fuel used in the afterburner was MIL-F-5572 unleaded gasoline having a lower heating value of 19,000 Btu per pound and a hydrogen-carbon ratio of 0.186.

[redacted]

Methods of calculating afterburner performance parameters are given in appendix A.

RESULTS AND DISCUSSION

During the afterburner performance investigation, trouble was encountered with "coke" or a hard carbon formation in the 3-ring fuel manifold. This coking tended to plug up some of the injection holes inside each of the manifold rings, but no remedy was found at this time. The plugged orifices altered the fuel distribution and therefore had an effect on afterburner performance. A study was made of the coking problem at the conclusion of the performance investigation in an attempt to determine the effect of the coke deposits on the performance and to prevent the formation of coke in the fuel manifold. Inasmuch as the coking problem modifies all the performance data, a discussion of the influence of coking on the afterburner characteristics precedes the performance data.

Characteristics of fuel manifold coking. - During most of the afterburner performance calibration, the standard cleaning procedure was to remove the afterburner fuel manifold and to drill the coke formation out of each of the plugged fuel-injection holes before running again with the manifold. However, near the end of the performance calibration, one of the manifolds was cut apart and was found to contain carbon flakes. This finding led to the conclusion that the drilling out of the injection holes was of little avail because the carbon flakes inside the manifold probably replugged the holes soon after fuel was run through the manifold.

Data indicating the extent of coking that was obtained during some of the performance calibration with all three fuel rings in operation are shown in the following table:

Coking run	Data points	Afterburner running time (hr)	Condition of fuel manifold after running, percent of orifices plugged		
			Outer	Middle	Inner
1	24	1.8	0.0	0.0	94.0
2	39	2.7	100.0	.0	84.0
3	10	.7	100.0	.0	100.0
4	15	1.0	.0	.0	17.0
5	27	1.6	.0	.0	.0

[redacted]

The fuel manifold used in runs 1 to 4 had been used previously during the afterburner calibration. Prior to each run the plugged fuel-injection holes were opened by drilling out the carbon formations. Although the fuel system was purged with air after each afterburner shutdown, there was some time lag between the shutdown and the purging. For run 5, for which a new fuel manifold was used, purging with about 25 pounds per square inch air was performed simultaneously with the afterburner shutdown.

It should be noted that the middle ring was free of coke deposits after each run, but that either the outer or inner fuel-manifold ring had some of the injection holes plugged after each of the runs except 5. The coking of the outer and inner fuel rings may have resulted from heat radiation from the annular flame-holder gutters which were very close to these rings, as shown in figure 3. Run 5 differed from the other runs in that the purging of the afterburner fuel lines with high-pressure air was performed simultaneously at every afterburner shutdown. From the data in the preceding table, it appears that if the purging operation with air is started at the same instant that the afterburner fuel is shut off, coke formation in the afterburner fuel system may be prevented.

Influence of fuel distribution on performance. - The afterburner was operated with different fuel-manifold-ring combinations to ascertain the effect on afterburner performance of plugged holes in the afterburner fuel manifold. A plot of engine net thrust as a function of total fuel flow is presented in figure 4(a). As previously stated, the turbine-outlet conditions were held constant by variations in exhaust-nozzle area; therefore changes in net thrust are indicative of changes in combustion efficiency for a given total fuel flow. For this comparison (run 5 in preceding table), coke formation was prevented by the instantaneous purging with air during every shutdown of the afterburner. Using the outer ring and then the inner ring of the afterburner fuel-injection manifold separately resulted in maximum net thrusts of about 1000 and 950 pounds, respectively, at relatively low total fuel flows. Operation with but one fuel ring resulted in poor fuel distribution and indicated that reasonable thrusts can be obtained only at low fuel flows. For higher thrust, more uniform fuel distribution would be needed at high fuel flows. With all three of the manifold rings in operation, a net thrust of about 1100 pounds was obtained at a fuel flow of 4000 pounds per hour. However, the fuel distribution was improved even more by the elimination of the middle ring; a net thrust of 1160 pounds was obtained at a fuel flow of 4800 pounds per hour. This comparison of thrusts with various ring combinations is evidence that the fuel-air distribution in the afterburner has an important effect on the thrust. A more detailed discussion of the effect of fuel distribution on afterburner performance is given in reference 1.

A comparison of 3-ring operation with and without coking in the fuel manifold is shown in figure 4(b). The thrust obtained with the clean manifold is about 8 percent higher than that with the "coked" manifold for the range of fuel flow shown. These data were obtained at an altitude of 40,000 feet and a flight Mach number of 0.52.

Comparison of performance calibration with "coked-manifold" data. - The data obtained during the performance calibration of the afterburner had an unknown degree of coking. These data are compared with the data obtained during run 2 of the coking study, which had coke deposits in the injection holes of both the inner and outer manifold rings (fig. 5). The data interplots for the four flight conditions shown, indicating the probability that there was some coking present in the fuel manifold for all the afterburner performance calibration data.

As a result, it would probably be possible to obtain somewhat higher thrusts and exhaust temperatures than are shown in the succeeding performance curves; however, the effects of changes in flight conditions on the trends in afterburner performance parameters subsequently shown are believed valid.

Performance Characteristics

Afterburner inlet conditions. - The condition of the engine exhaust gases entering the afterburner was held reasonably constant for a given flight condition. By varying the exhaust-nozzle area it was possible to obtain data over a wide range of afterburner fuel-air ratio with a maximum variation in turbine-outlet temperature of approximately 100° F (fig. 6(a)). The 100° temperature variation at the turbine outlet was due primarily to differences in the temperature distribution in the plane of the engine control thermocouples. For instance, a turbine-outlet temperature of about 1740° R was obtained at both 10,000 and 25,000 feet, whereas a temperature of 1665° R was obtained at an altitude of 40,000 feet (fig. 6(a)). The average velocity of the gases $3\frac{1}{2}$ inches upstream of the flame holder was about 480 feet per second for all conditions.

In addition to the deviation in turbine-outlet temperature at 40,000 feet (flight Mach number, 0.52), the compressor-inlet temperature was about 40° above NACA standard altitude conditions. If the engine-inlet and turbine-outlet temperatures were correct, the temperature ratio across the engine would have been about 4.2 instead of 3.6, as it was at this flight condition. The increased engine temperature ratio would result in a turbine-outlet pressure about 12 percent higher than was obtained. However, because the increase in turbine-outlet pressure between 40,000 and 25,000 feet is 113 percent, the 12-percent

error in turbine-outlet pressure at the high altitude would have only a secondary effect on the altitude trends shown. An increase in turbine-outlet pressure would tend to improve the combustion efficiency and the specific fuel consumption, but would have little effect on the thrust augmentation ratio because both the normal engine and the afterburner thrust would be increased slightly.

Effect of altitude and flight Mach number. - Turbine-outlet temperature, combustion efficiency, exhaust-gas temperature, thrust augmentation ratio, and specific fuel consumption are shown as functions of afterburner fuel-air ratio in figure 6 for three altitudes at constant flight Mach number and in figure 7, for three flight Mach numbers at constant altitude.

Increasing the altitude from 10,000 to 40,000 feet lowered the maximum obtainable afterburner combustion efficiency from 0.95 to 0.60 at exhaust-gas temperatures of 3000° and 2900° R, respectively (fig. 6(b)). In addition, the same change in altitude raised the afterburner fuel-air ratio required for a given exhaust-gas temperature or thrust augmentation ratio (figs. 6(c) and 6(d)). The exhaust-nozzle area was too small to obtain maximum thrust at 10,000 feet, as evidenced by the fact that the thrust augmentation curve is still increasing at the highest afterburner fuel-air ratio.

For most afterburner fuel-air ratios, increasing the ram pressure ratio (fig. 7), which resulted in higher afterburner pressures, increased the afterburner combustion efficiency, lowered the specific fuel consumption, and increased exhaust-gas temperature and thrust augmentation ratio. The change in both combustion efficiency and specific fuel consumption with altitude and flight Mach number at a given exhaust-gas temperature correlates with the change in turbine-outlet pressure; that is, the improvement in combustion efficiency and specific fuel consumption with an increase in flight speed or a decrease in altitude is simply a function of the change in turbine-outlet pressure.

By cross plotting the curves in figures 6 and 7, the variation of combustion efficiency, thrust augmentation ratio, and specific fuel consumption with altitude and flight Mach number was obtained at constant exhaust-gas temperatures (figs. 8 and 9). For a given altitude, changes in exhaust temperature had little effect on the afterburner combustion efficiency (fig. 8(a)). It should be noted that exhaust-gas temperature changes had no effect on the pressure in the afterburner (disregarding the momentum pressure loss) because the turbine-outlet conditions were maintained constant by varying the exhaust-nozzle area. However, both the net-thrust augmentation ratio and specific fuel consumption increased considerably as the exhaust-gas temperature was raised (figs. 8(b) and (c)). The net thrust

increase results from the increase in exhaust-gas velocity; the specific fuel consumption increases because a larger percentage of the total fuel flow is burned in the afterburner where the cycle efficiency is relatively low. The thrust augmentation curves increase with flight Mach number at constant exhaust-gas temperature (fig. 9(b)). This increase results from the increase in the inlet momentum term (as flight Mach number is increased), which is subtracted from the jet thrust of both the normal and augmented engines (see thrust equations in appendix A).

As previously mentioned, the effects of variable fuel distribution associated with coking deposits in the fuel manifold decreased the net thrust as much as 8 percent; however, the effects of changes in flight conditions on the magnitude of the trends of the performance parameters are believed to be valid.

Operational Characteristics

Afterburner pressure losses. - The total-pressure loss in the afterburner (summation of friction and momentum pressure loss) is plotted as a function of exhaust-gas temperature for several altitudes and flight Mach numbers in figure 10. Afterburner total-pressure losses between 5 and 6 percent were obtained without afterburning (exhaust-gas temperature about 1700° R); increasing the exhaust temperature to 3200° R raised the total-pressure loss about $3\frac{1}{2}$ percentage points. This increased pressure loss is a result of the momentum pressure loss due to the addition of heat. The difference in the friction pressure loss for various flight conditions is a result of slight differences in the Mach number at the entrance to the afterburner.

Afterburner ignition and blow-out. - Ignition of the afterburner was accomplished by injecting an extra portion of fuel in the engine combustion chamber, which resulted in a flash of flame through the turbine and into the afterburner. This system worked very well for all flight conditions except the low flight speeds at high altitudes. For instance, at 40,000 feet a flight Mach number of about 0.5 was required before the afterburner could be ignited.

The effect of flight speed and altitude on the operable afterburner fuel-air-ratio range is shown in figure 11. Decreased afterburner pressure (which corresponds to an increase in altitude or a decrease in flight Mach number) resulted in lean blow-out occurring at higher afterburner fuel-air ratios. Afterburner blow-out due to excessively high fuel-air ratios was not obtained. The blow-out, shown in terms of altitude and flight speed, correlates with turbine-outlet pressure; that is, the data fall on a single curve when plotted against turbine-outlet pressure.

SUMMARY OF RESULTS

An investigation of the Westinghouse XJ34-WE-32 engine with the production afterburner in the altitude wind tunnel yielded the following results:

1. Reproducible afterburner performance was difficult to obtain because of "coking" or carbon deposits in the injection holes of the production fuel manifold in the afterburner. At an altitude of 40,000 feet, a thrust difference of 8 percent was obtained between a clean and a coked fuel manifold.

2. For the limited running time of this investigation, no coking deposits were formed in the fuel manifold when the afterburner fuel system was purged with high-pressure air at the same time the afterburner was shut off.

3. At a Mach number of 0.52 and an altitude of 40,000 feet, higher thrust could be obtained at a given total fuel flow by blocking out the middle ring of the 3-ring fuel-injection manifold.

4. Changes in altitude and flight Mach number had the normal effects on the afterburning performance parameters; that is, increased pressure in the afterburner raised the combustion efficiency and lowered the specific fuel consumption. Although reasonable combustion efficiencies were obtained at 10,000 feet (maximum about 95 percent at an exhaust temperature of 3000° R), the exhaust-nozzle area was too small to obtain maximum thrust. At an altitude of 40,000 feet, the peak combustion efficiency was 60 percent at an exhaust temperature of 2900° R.

5. Ignition of the afterburner was accomplished by injecting an extra portion of fuel into the engine combustion chamber, which resulted in a flash of flame through the turbine and into the afterburner. This system worked at all flight conditions except low air speeds at the higher altitudes.

Lewis Flight Propulsion Laboratory
National Advisory Committee for Aeronautics
Cleveland, Ohio

APPENDIX A

METHODS OF CALCULATION

Temperatures. - Static temperatures were determined from indicated temperatures with the following relation:

$$t = \frac{T_1}{1 + 0.85\left[\left(\frac{P}{p}\right)^{\frac{\gamma-1}{\gamma}} - 1\right]} \tag{1}$$

where 0.85 is the impact recovery factor for the type of thermocouple used. Total temperature was calculated by the adiabatic relation between temperatures and pressures. (The symbols are defined in appendix B.)

Flight Mach number. - Flight Mach number was calculated from ram pressure ratio by the following equation assuming complete pressure recovery at the engine inlet:

$$M_0 = \sqrt{\frac{2}{\gamma-1}\left[\left(\frac{P_1}{p_0}\right)^{\frac{\gamma-1}{\gamma}} - 1\right]} \tag{2}$$

Airspeed. - The equivalent airspeed was calculated using the equation

$$V_0 = M_0\sqrt{\gamma g R T_1 \left(\frac{p_0}{P_1}\right)^{\frac{\gamma-1}{\gamma}}} \tag{3}$$

Air flow. - Air flow was determined from pressure and temperature measurements in the engine-inlet air duct by the equation

$$W_{a_1} = p_1 A_1 \sqrt{\frac{2\gamma_1 g}{(\gamma_1-1)Rt_1}\left[\left(\frac{P_1}{p_1}\right)^{\frac{\gamma_1-1}{\gamma_1}} - 1\right]} \tag{4}$$

Gas flow. - The total weight flow through the engine and afterburner was calculated as follows:

$$\left.\begin{aligned} \text{(Engine)}\quad W_{g_5} &= W_{a_1} + \frac{W_{f_e}}{3600} \\ \text{(Afterburner)}\quad W_{g_8} &= W_{a_1} + \frac{\left(W_{f_e} + W_{f_{ab}}\right)}{3600} \end{aligned}\right\} \qquad (5)$$

Afterburner fuel-air ratio. - The afterburner fuel-air ratio is defined as the ratio of the weight flow of fuel injected into the afterburner to the weight flow of unburned air entering the afterburner from the engine. Weight flow of unburned air was determined by assuming the fuel injected into the engine combustor was completely burned therein. The fuel-air ratio is

$$(f/a)_{ab} = \frac{W_{f_{ab}}}{3600\ W_{a_1} - \left(\frac{W_{f_e}}{0.068}\right)} \qquad (6)$$

where 0.068 is the stoichiometric fuel-air ratio for the engine fuel.

Combustion efficiency. - Afterburner combustion efficiency was obtained by dividing the enthalpy rise through the afterburner by the product of the afterburner fuel flow and the lower heating value of the afterburner fuel, disregarding dissociation of the exhaust gas:

$$\eta_{b_{ab}} = \frac{3600\ W_g\ \Delta H_{ab}}{W_{f_{ab}}\ h_{c_{ab}}}$$

$$= \frac{3600\ W_{a_1} \left[H_a\right]_{T_2}^{T_8} + W_{f_e} \left[H_{f_e}\right]_{T_b}^{T_8} + W_{f_{ab}} \left[H_{f_{ab}}\right]_{T_b}^{T_8} - \eta_{b_e}\ W_{f_e}\ h_{c_e}}{W_{f_{ab}}\ h_{c_{ab}} + W_{f_e}\ h_{c_e} - \eta_{b_e}\ W_{f_e}\ h_{c_e}} \qquad (7)$$

The enthalpy of the products of combustion was determined from a chart using the hydrogen-carbon ratio and temperature as explained in reference 2.

Augmented thrust. - The jet thrust of the installation was determined from the balance-scale measurements by the following equation:

$$F_{j_s} = B + D + D_r + \frac{W_{a_1} V_1}{g} + A_X(p_1 - p_0) \tag{8}$$

The last two terms of this expression represent the momentum and pressure forces on the installation at the slip joint in the inlet-air duct. The external drag of the installation was determined with the engine inoperative. Drag of the water-cooled exhaust-nozzle survey rake was measured by an air-balance piston mechanism.

Scale net thrust was obtained by subtracting the equivalent free-stream momentum of the inlet air from the scale jet thrust:

$$F_{n_s}' = F_{j_s} - \frac{W_{a_1} V_0}{g} \tag{9}$$

Velocity coefficient. - The velocity coefficient, determined from tests with the afterburner inoperative, is defined as the ratio of scale jet thrust to rake jet thrust,

$$C_V = \frac{F_{j_s}}{F_{j_8}}$$

Rake jet thrust F_{j_8} is given by the following equation based on exhaust-nozzle-outlet total pressure and temperature using the charts presented in reference 3:

$$F_{j_8} = \frac{W_{g_8}}{g} V_n + A_n(p_n - p_0) \tag{10}$$

Normal engine thrust. - Normal engine thrust is the theoretical thrust that would be obtained with the engine and a standard-engine tail pipe equipped with a nozzle of a size that gives the same turbine-outlet pressures and temperatures as were encountered with afterburning under the same flight conditions. The normal thrust of the engine was calculated from measurements during the afterburning program of total pressure and temperature at the turbine outlet, gas flow at the turbine outlet, and from previously determined total-pressure loss across the standard tail pipe using the charts presented in reference 3:

$$F_{n_e} = C_V\left[\frac{W_{g_5}}{g} V_n + A_n(p_n - p_0)\right] - \frac{W_{a_1} V_0}{g} \qquad (11)$$

A value of unity was assumed for the velocity coefficient C_V used in equation (11). Experimental data indicated that the total-pressure loss through the standard tail pipe was approximately 0.01 P_5 at rated engine speed.

Augmented net-thrust ratio is defined as

$$\frac{\text{Scale net thrust, } F_{n_s}}{\text{Normal engine net thrust, } F_{n_e}}$$

Exhaust-gas total temperature. - The total temperature of the exhaust gas was calculated from the exhaust-nozzle-outlet total pressure, augmented scale jet thrust, velocity coefficient, and gas flow by means of the following equation:

$$T_j = \left(\frac{F_{j_s}}{C_V}\right)^2 \frac{\gamma_8 - 1}{2\gamma_8} \frac{g}{R(W_{g_8})^2} \left[\frac{1}{1 - \left(\frac{p_0}{p_8}\right)^{\frac{\gamma_8 - 1}{\gamma_8}}}\right] \qquad (12)$$

APPENDIX B

SYMBOLS

The following symbols are used in the calculations and on the figures:

A	cross-sectional area, sq ft
B	thrust scale reading, lb
C_V	velocity coefficient, ratio of scale jet thrust to rake jet thrust
D	external drag of installation, lb
D_r	drag of exhaust-nozzle survey rake, lb
F_j	jet thrust, lb
F_n	net thrust, lb
f/a	fuel-air ratio
g	acceleration due to gravity, 32.2 ft/sec^2
H	total enthalpy, Btu/lb
h_c	lower heating value of fuel, Btu/lb
M	Mach number
P	total pressure, lb/sq ft absolute
p	static pressure, lb/sq ft absolute
R	gas constant, 53.4 ft-lb/(lb)(^oR)
T	total temperature, ^oR
t	static temperature, ^oR
V	velocity, ft/sec
W_a	air flow, lb/sec
W_f	fuel flow, lb/hr

W_f/F_n specific fuel consumption based on total fuel flow and net thrust, lb/(hr)(lb thrust)

W_g gas flow, lb/sec

γ ratio of specific heat for gases

η_b combustion efficiency

Subscripts:

a air

ab afterburner

b base temperature of 540° R

e engine

f fuel

i indicated

j jet

n exhaust-nozzle exit

s scale

X inlet duct at frictionless slip joint

0 free-stream conditions

1 engine-inlet duct

2 compressor-inlet annulus

5 afterburner inlet (turbine outlet)

8 exhaust nozzle, $1\frac{3}{8}$ inches forward of fixed portion of exhaust-nozzle outlet

REFERENCES

1. Fleming, W. A., Conrad, E. William, and Young, A. W.: Experimental Investigation of Tail-Pipe-Burner Design Variables. NACA RM E50K22, 1951.

2. Turner, L. Richard, and Lord, Albert M.: Thermodynamic Charts for the Computation of Combustion and Mixture Temperatures at Constant Pressure. NACA TN 1086, 1946.

3. Turner, L. Richard, Addie, Albert N., and Zimmerman, Richard H.: Charts for the Analysis of One-Dimensional Steady Compressible Flow. NACA TN 1419, 1948.

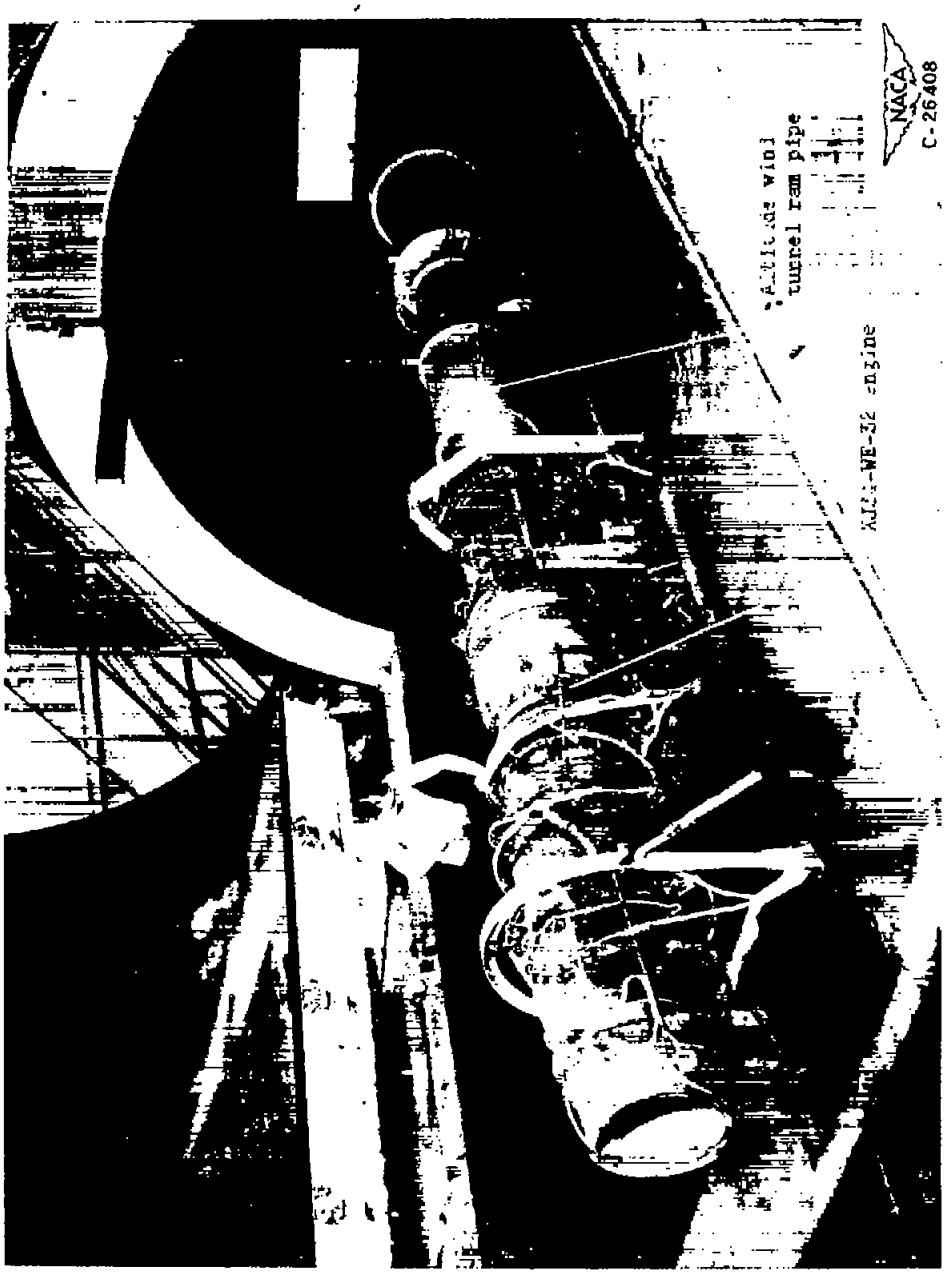

Figure 1. - Installation of Westinghouse XJ34-WE-32 engine in altitude wind tunnel.

Station	Total-pressure tubes	Static-pressure tubes	Thermo-couples
1	17	5	9
2	16	10	8
3	15	3	3
4	5	-	-
5	21	3	36
8	9	7	-

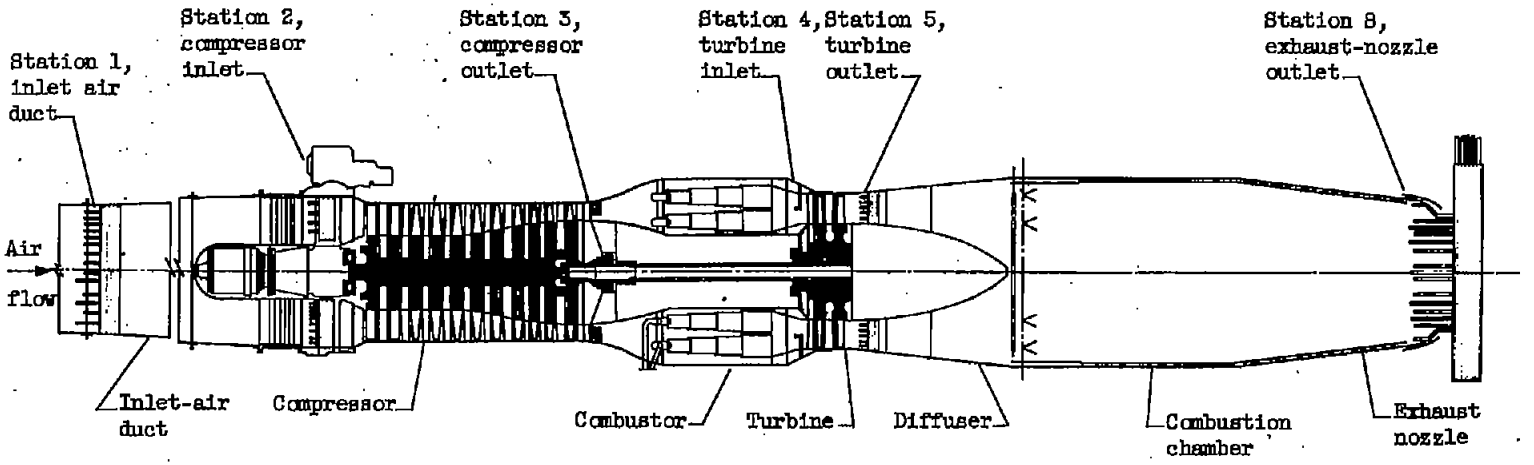

Figure 2. - Cross section of engine showing location of instrumentation.

Afterburner fuel-manifold ring	Ring diameter (in.)	Number of injection holes	Hole diameter (in.)
A	21	72	0.031
B	$16\frac{3}{4}$	64	.029
C	$14\frac{5}{8}$	32	.028

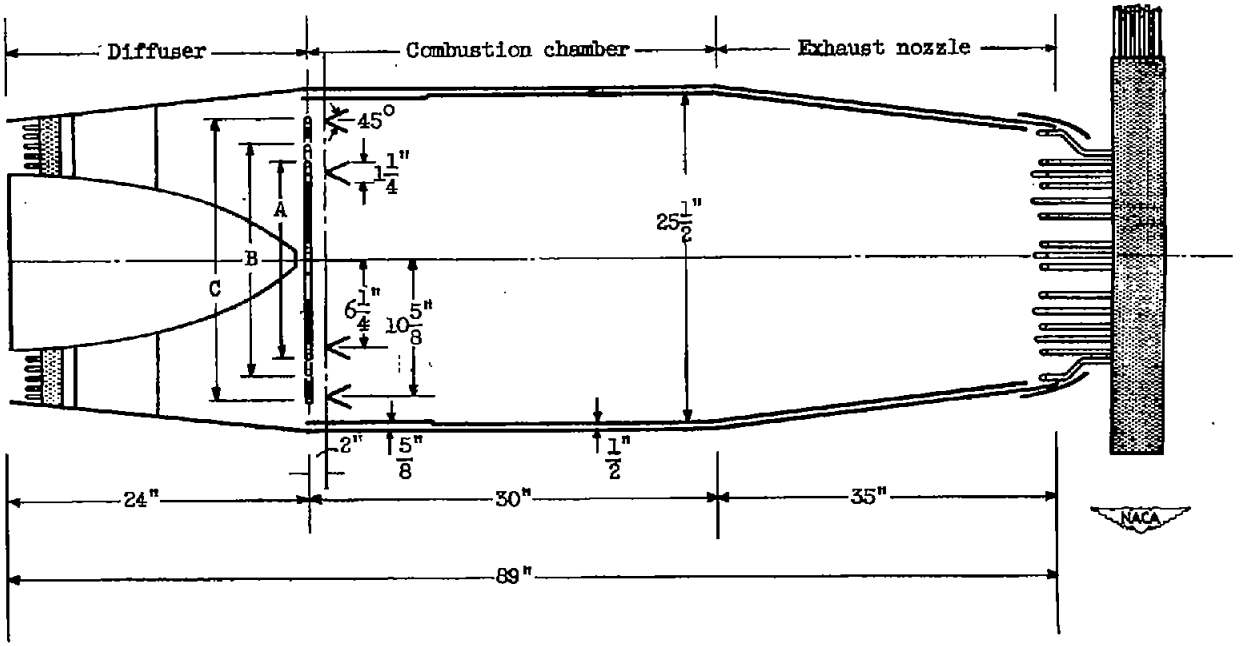

Figure 3. - Cross-section of afterburner.

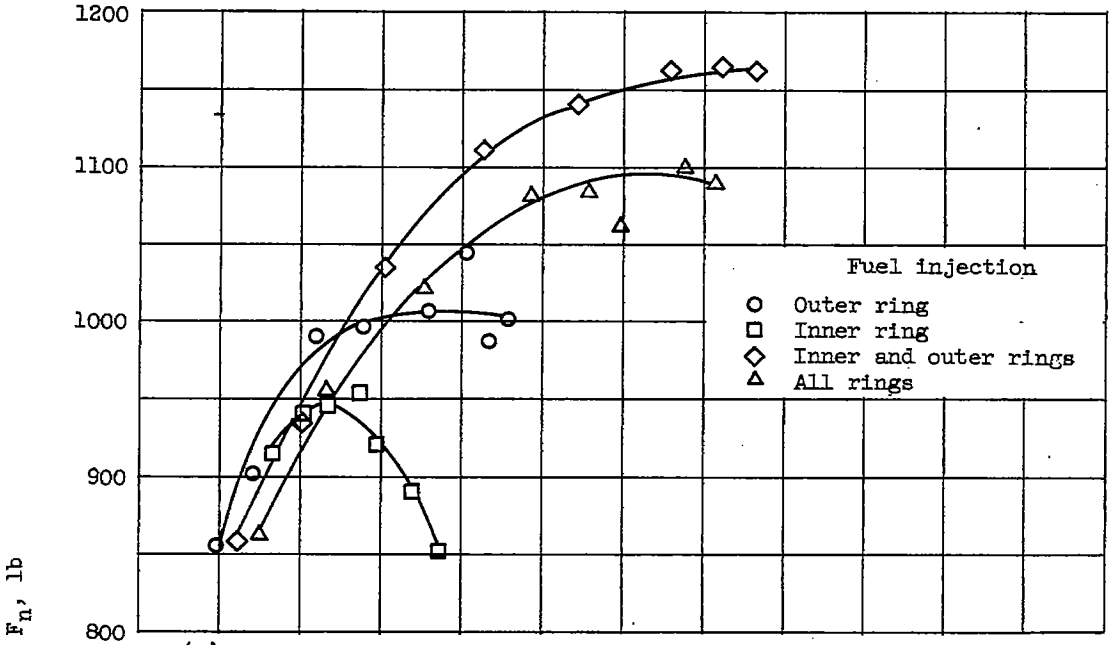

(a) Thrust with various fuel-manifold-ring combinations in operation; data from run 5.

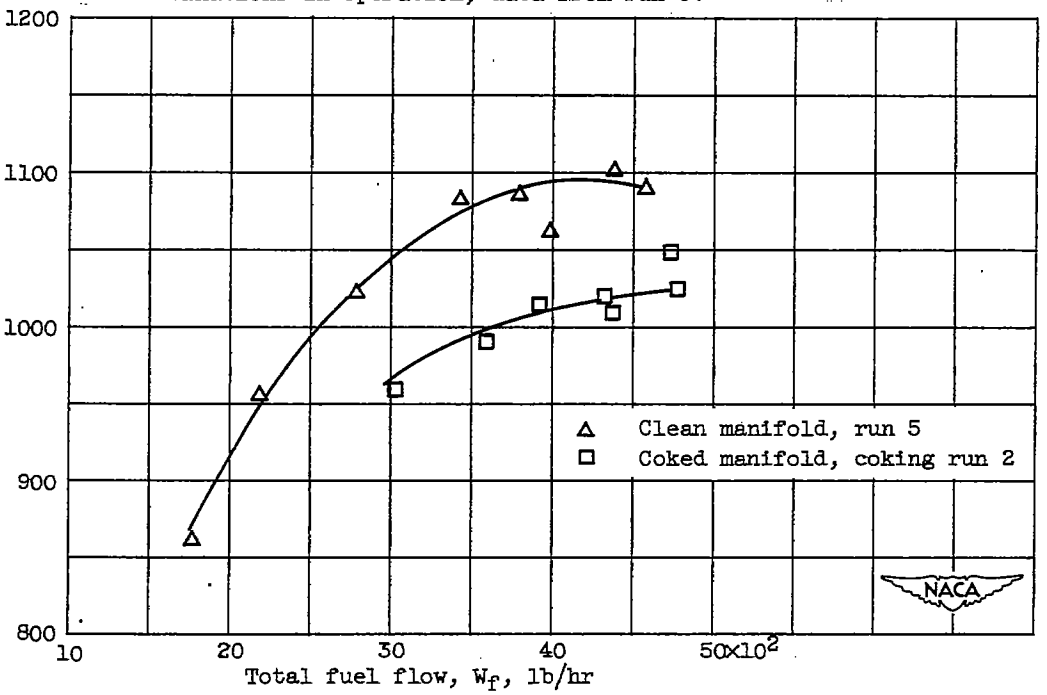

(b) Thrust with and without fuel manifold coking (all 3 rings).

Figure 4. - Effect of operation with various fuel-manifold-ring combinations and fuel manifold coking on afterburner net thrust. Altitude, 40,000 feet; flight Mach number, 0.52.

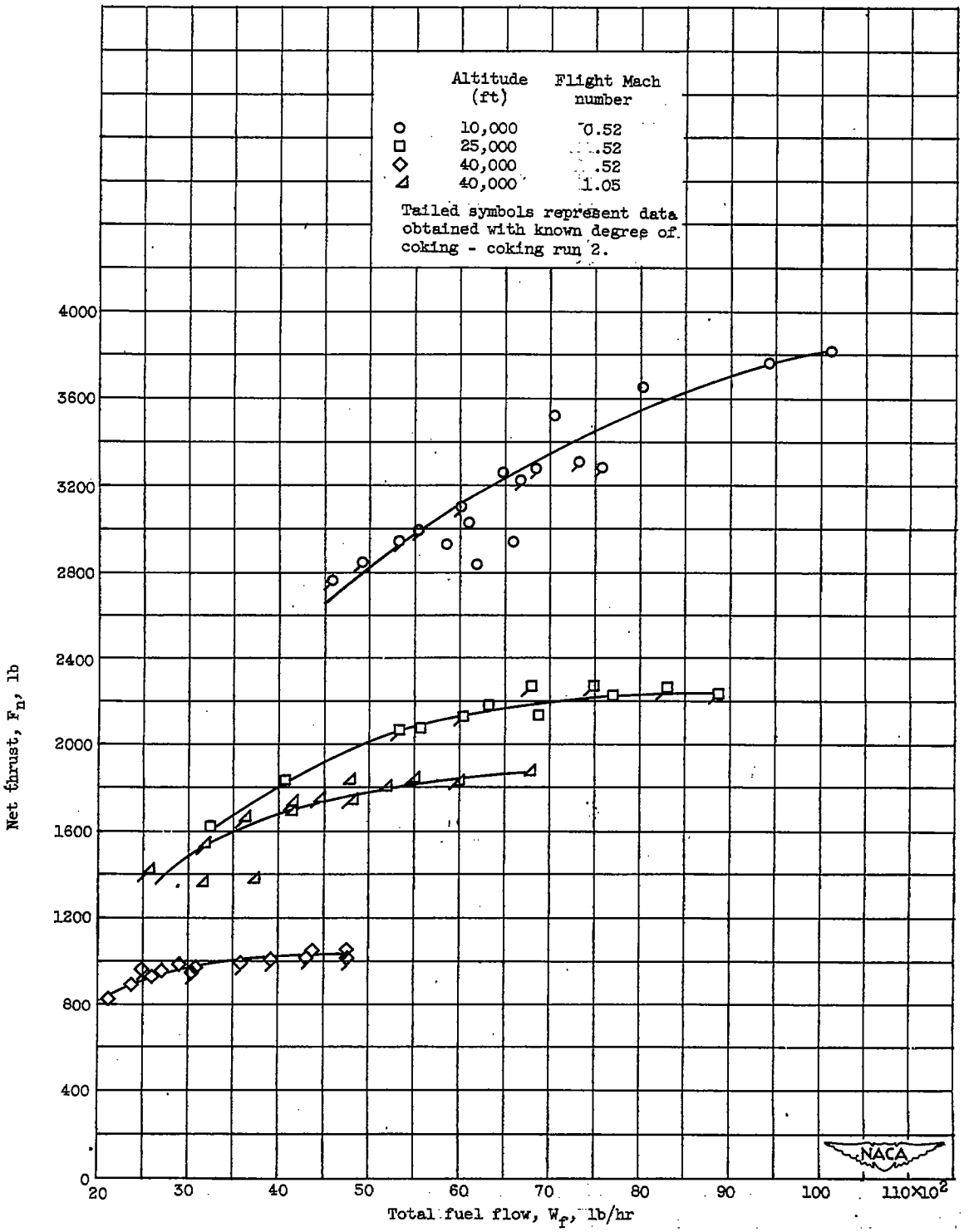

Figure 5. - Comparison of data obtained during performance calibration with data obtained during coking study for fuel manifold with a known degree of coking.

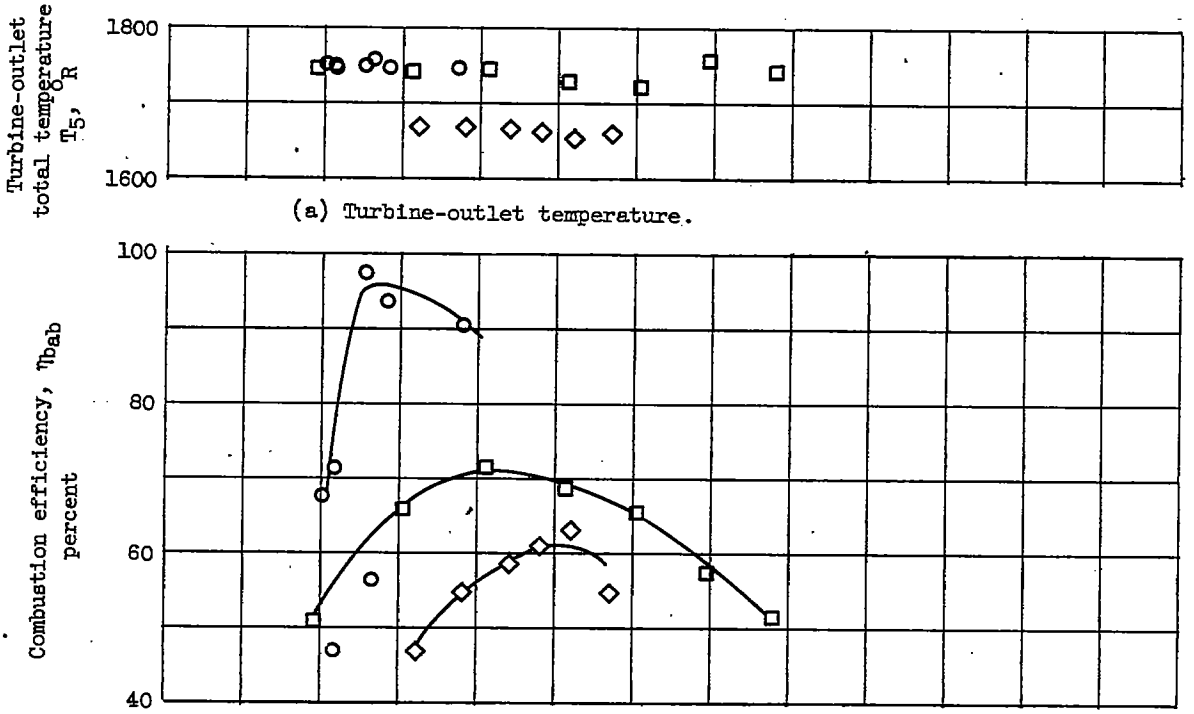

(a) Turbine-outlet temperature.

(b) Combustion efficiency.

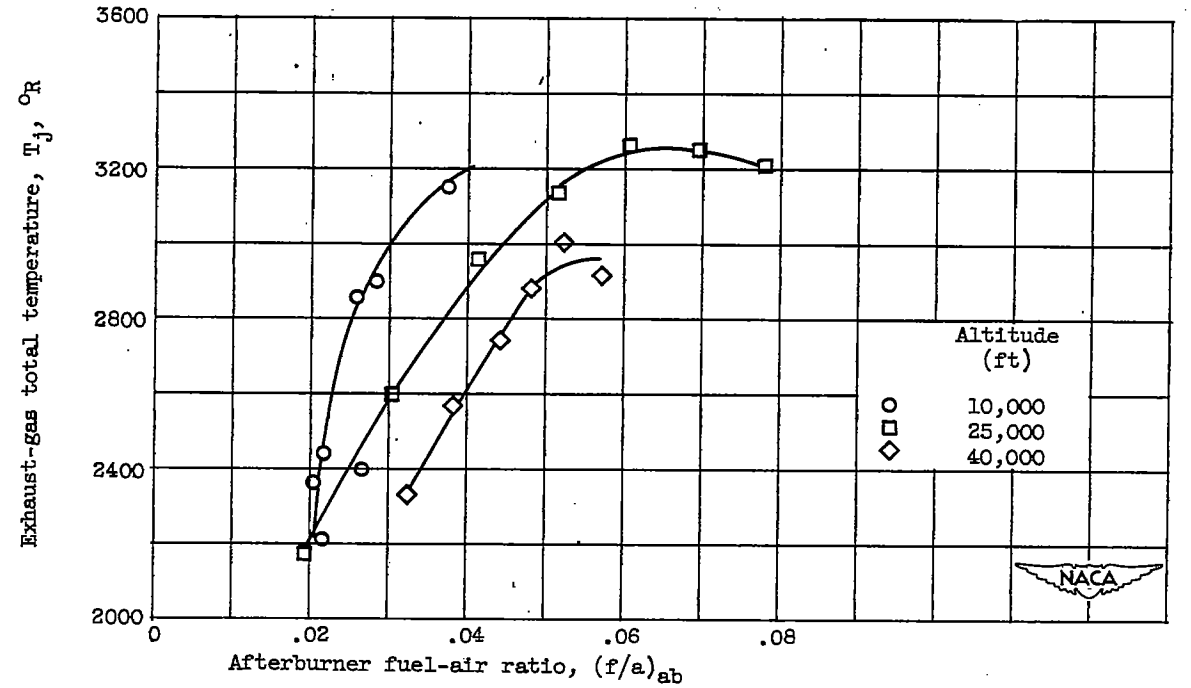

(c) Exhaust-gas temperature.

Figure 6. - Effect of altitude on variation of afterburner performance parameters with afterburner fuel-air ratio at flight Mach number of 0.52.

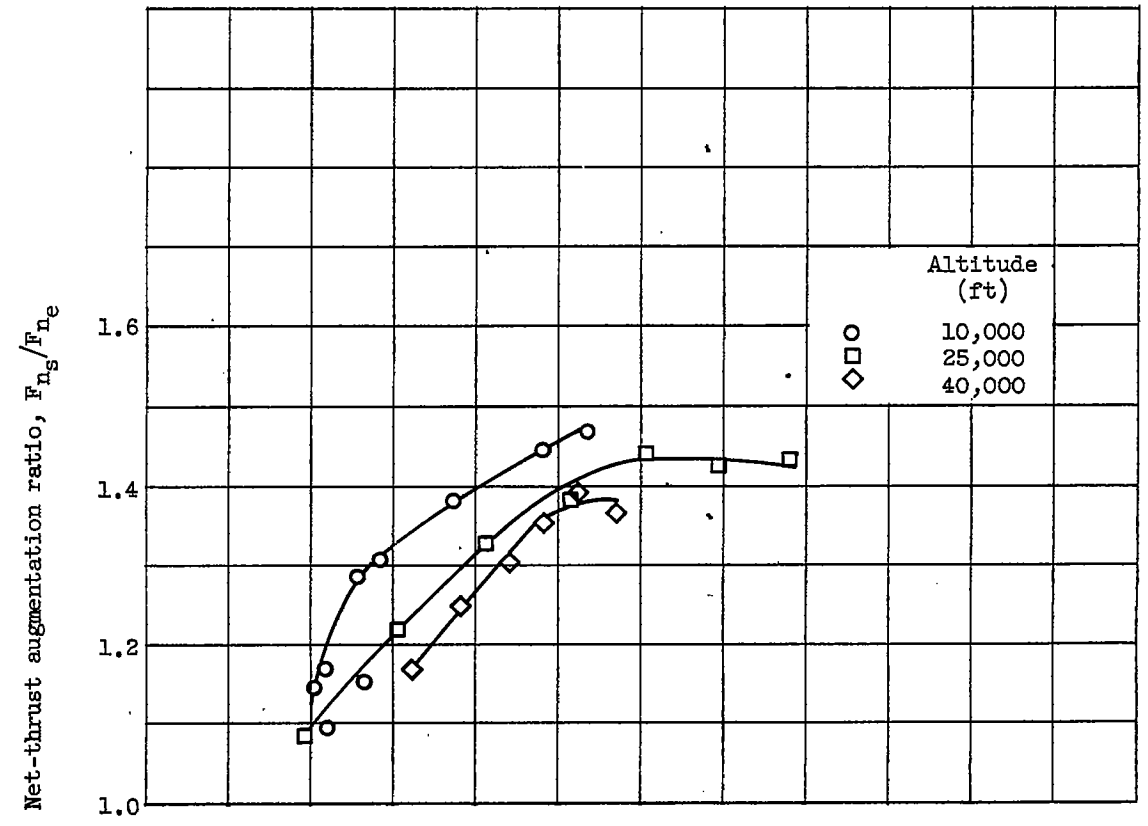

(d) Thrust augmentation ratio.

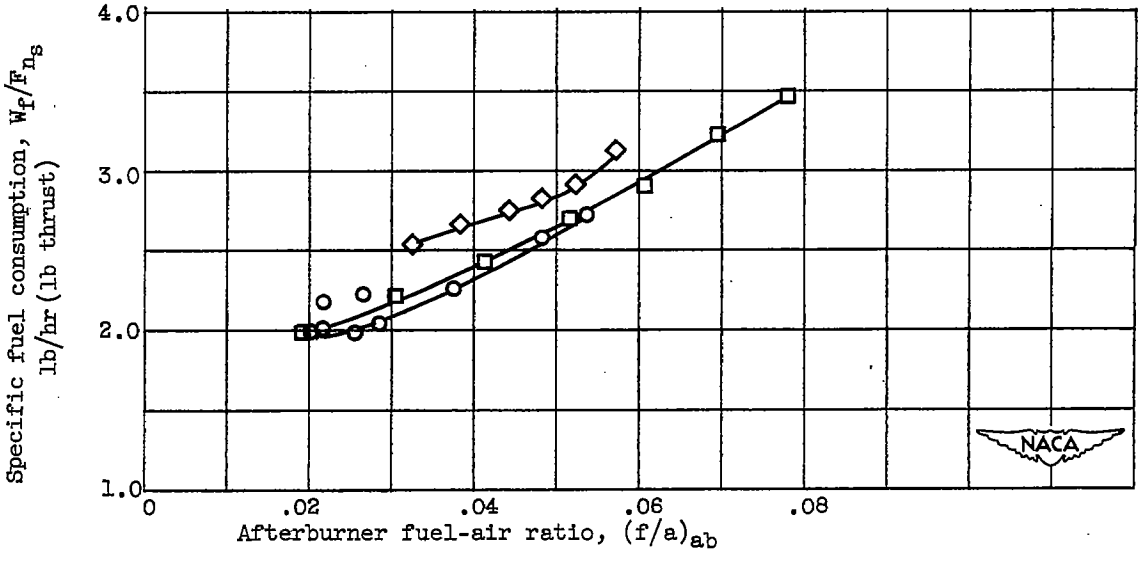

(e) Specific fuel consumption.

Figure 6. - Concluded. Effect of altitude on variation of afterburner performance parameters with afterburner fuel-air ratio at flight Mach number of 0.52.

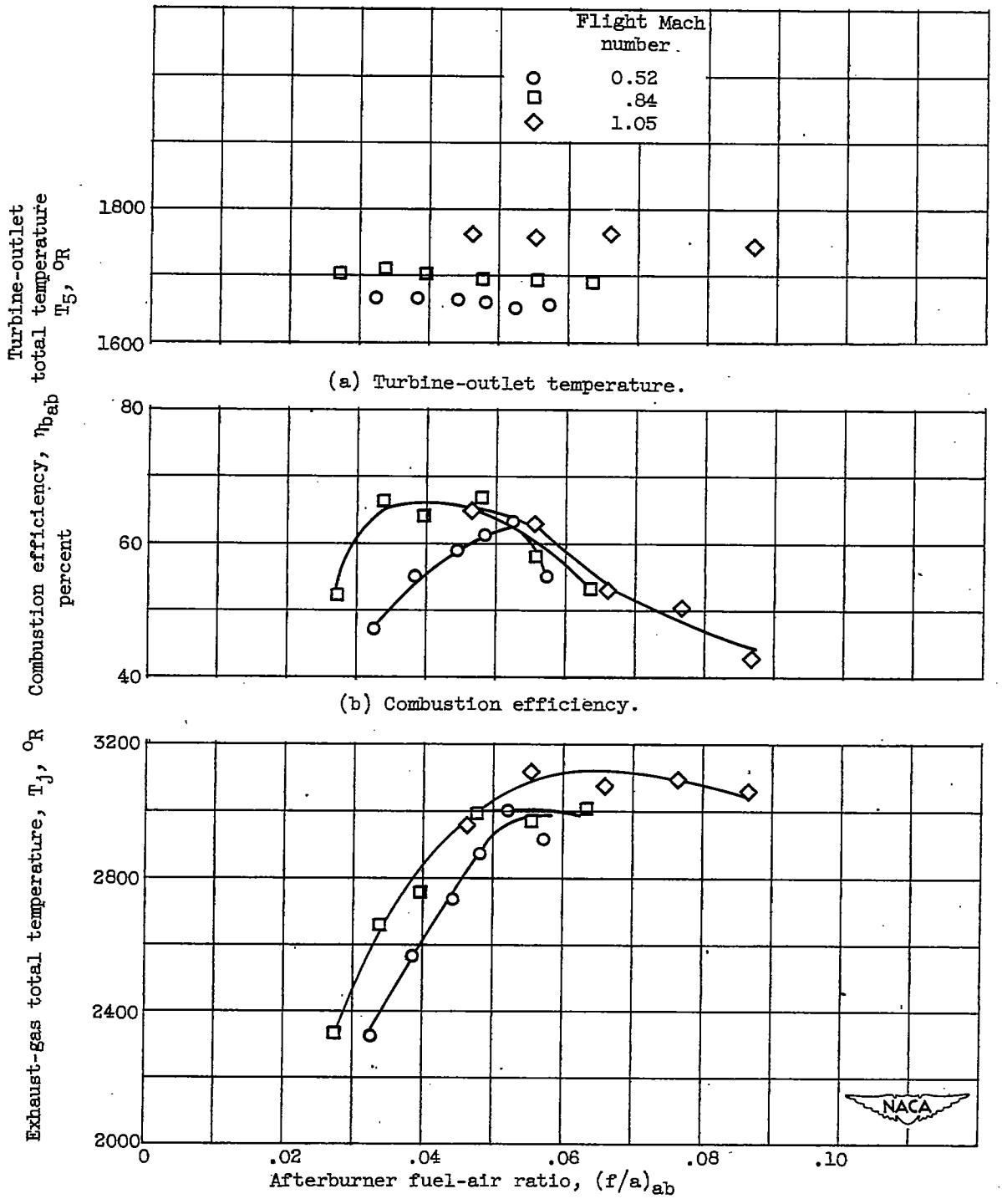

Figure 7. - Effect of flight Mach number on variation of afterburner performance parameters with afterburner fuel-air ratio at altitude of 40,000 feet.

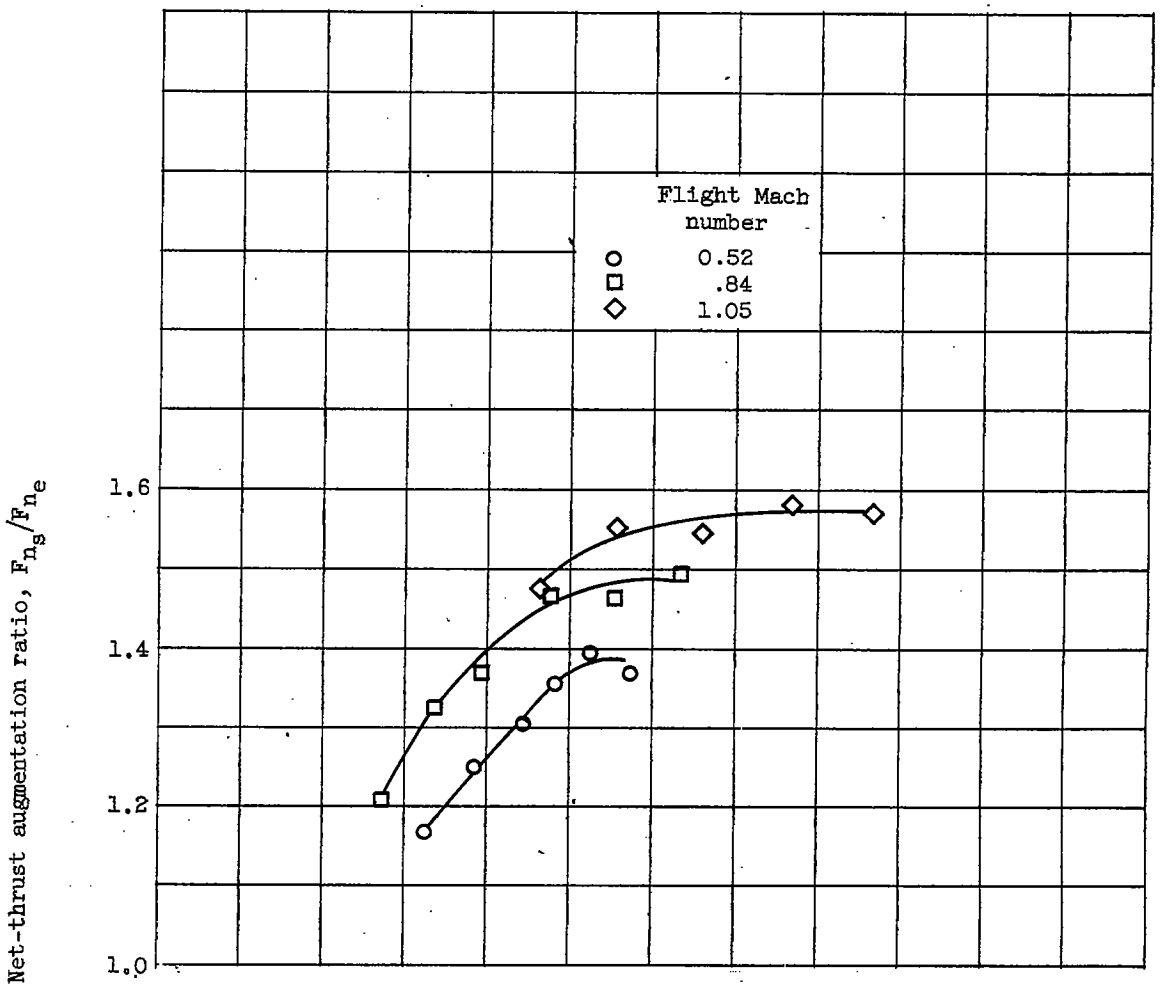

(d) Thrust augmentation ratio.

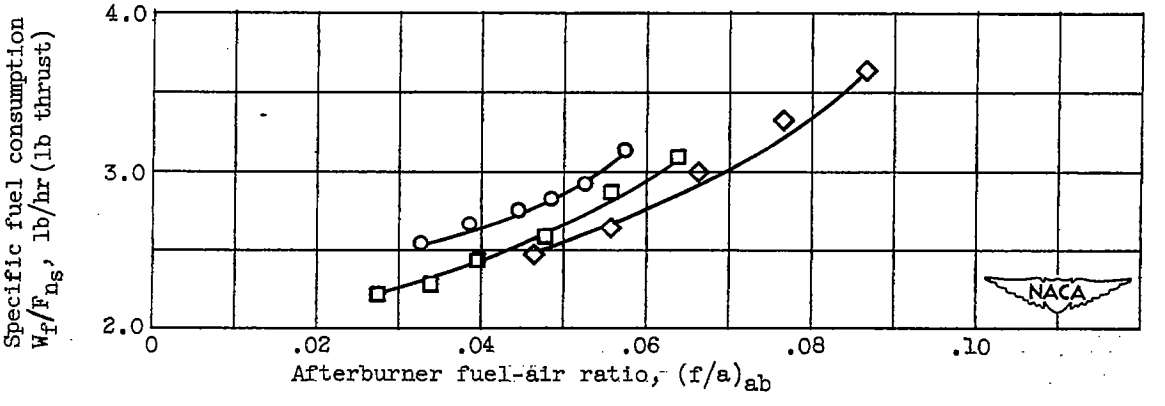

(e) Specific fuel consumption.

Figure 7. - Concluded. Effect of flight Mach number on variation of afterburner performance parameters with afterburner fuel-air ratio at altitude of 40,000 feet.

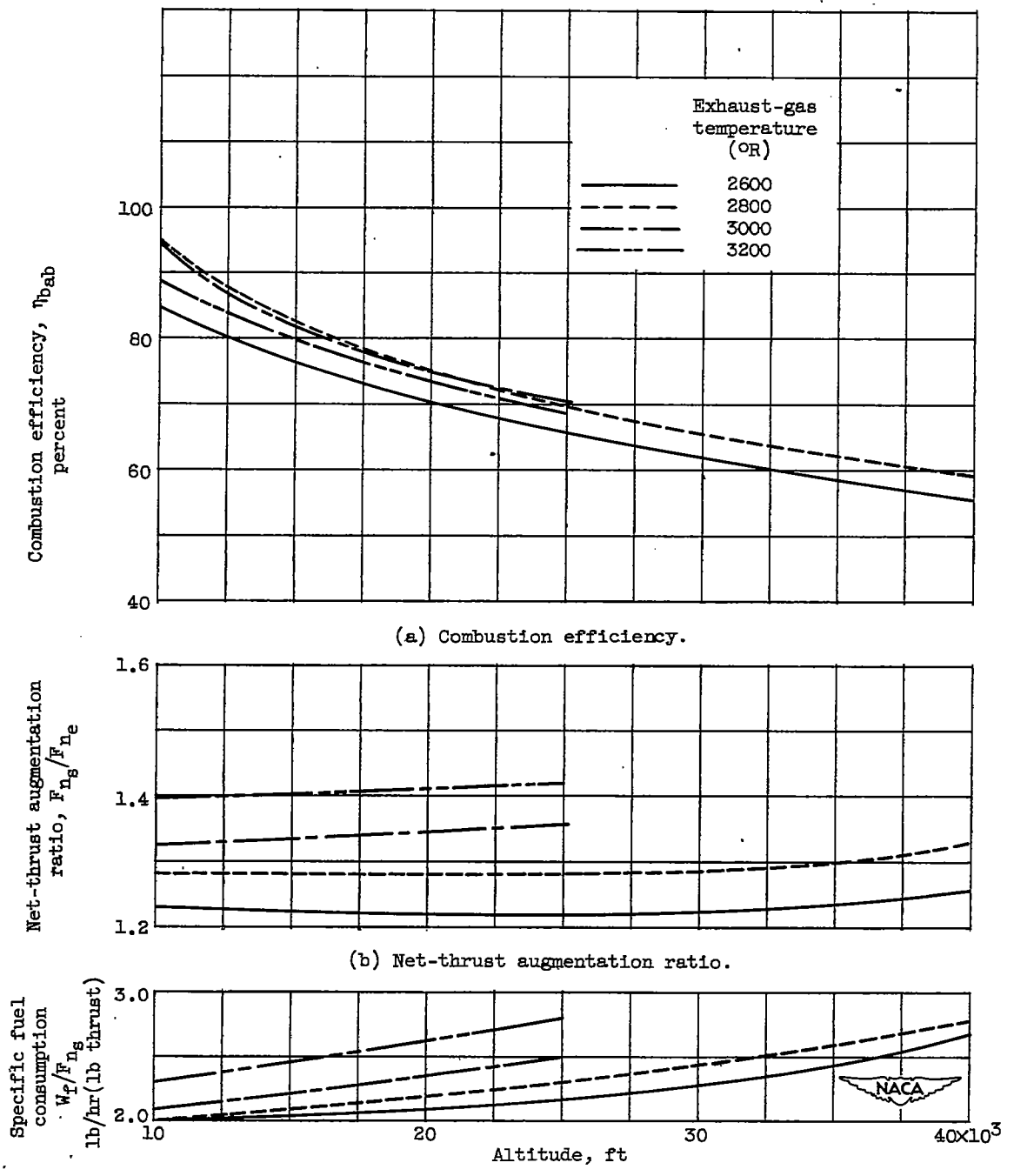

Figure 8. - Effect of exhaust-gas temperature on variation of afterburner performance parameters with altitude at flight Mach number of 0.52.

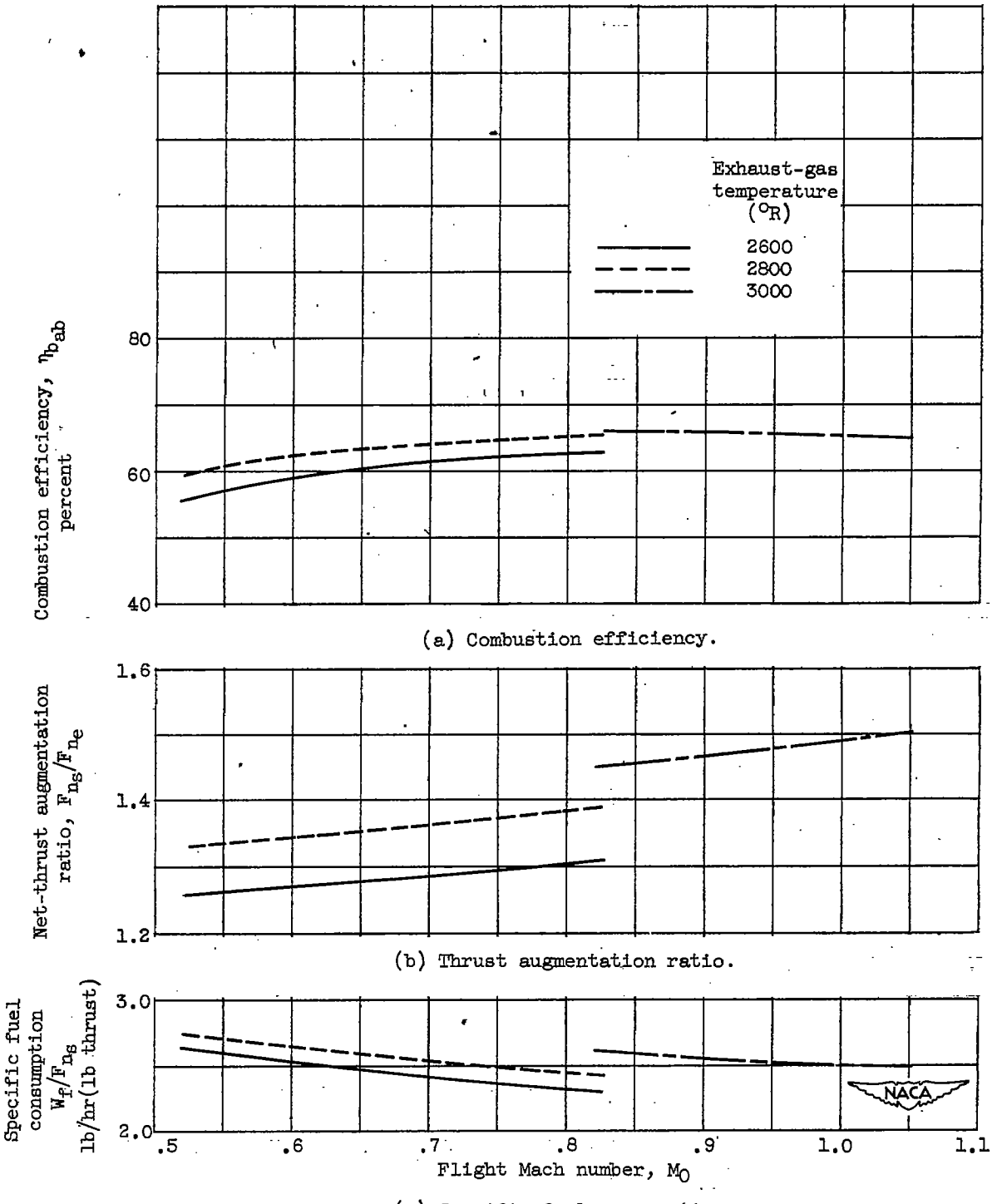

Figure 9. - Effect of exhaust-gas temperature on variation of afterburner performance parameters with flight Mach number at altitude of 40,000 feet.

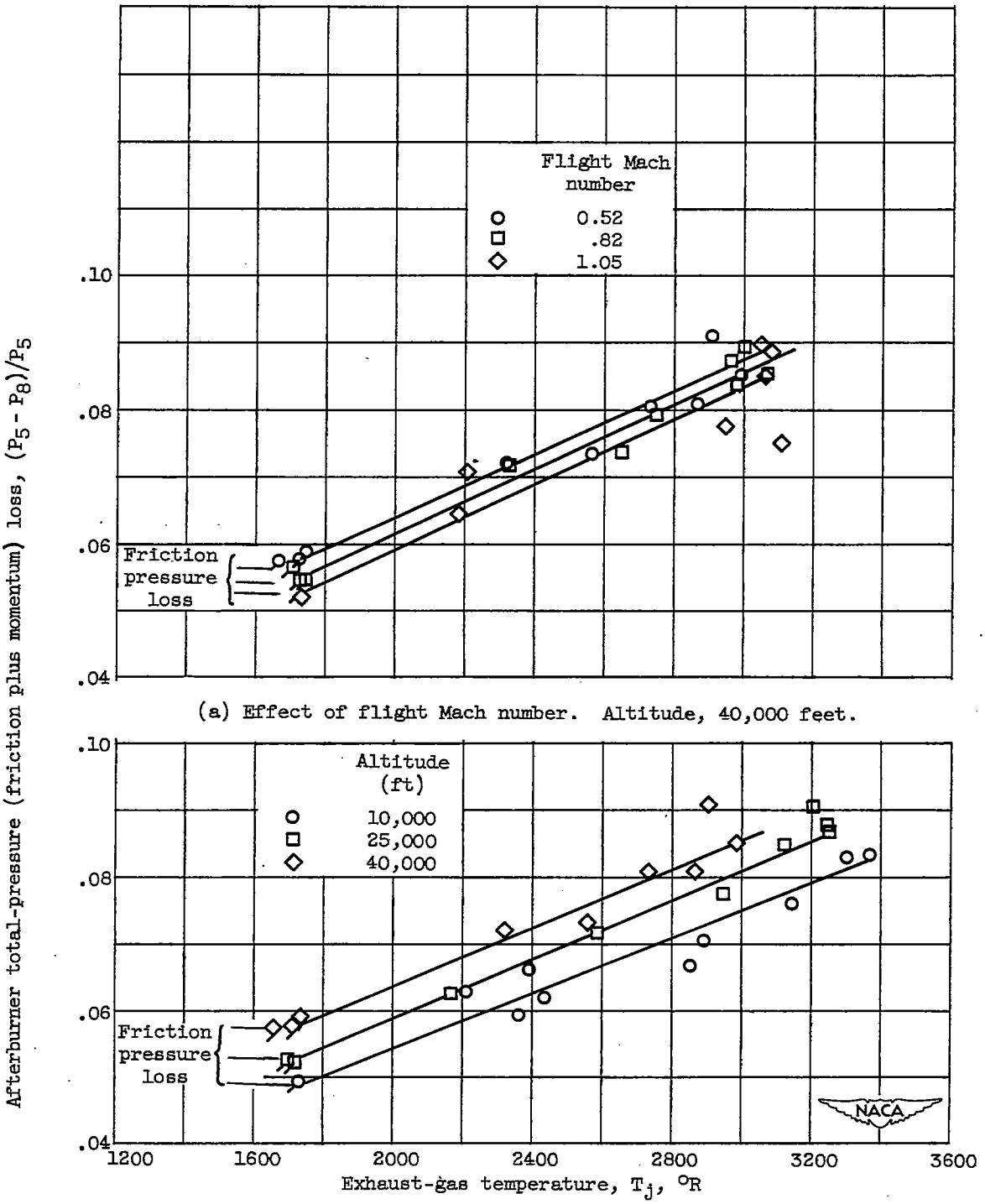

(a) Effect of flight Mach number. Altitude, 40,000 feet.

(b) Effect of altitude.

Figure 10. - Variation of afterburner total-pressure loss with exhaust-gas temperature. Tailed symbols indicate afterburner inoperative.

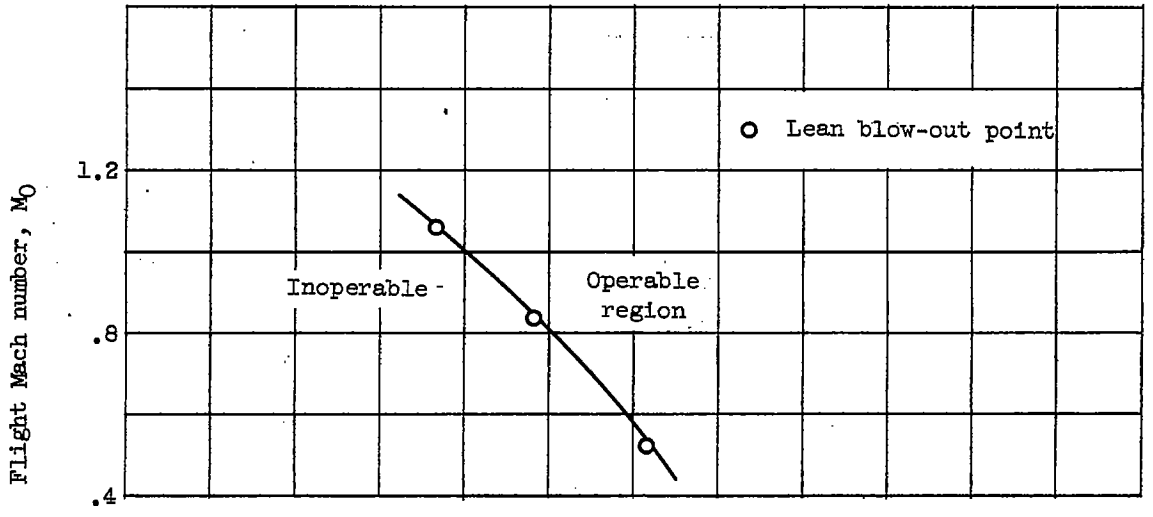

(a) Altitude, 40,000 feet.

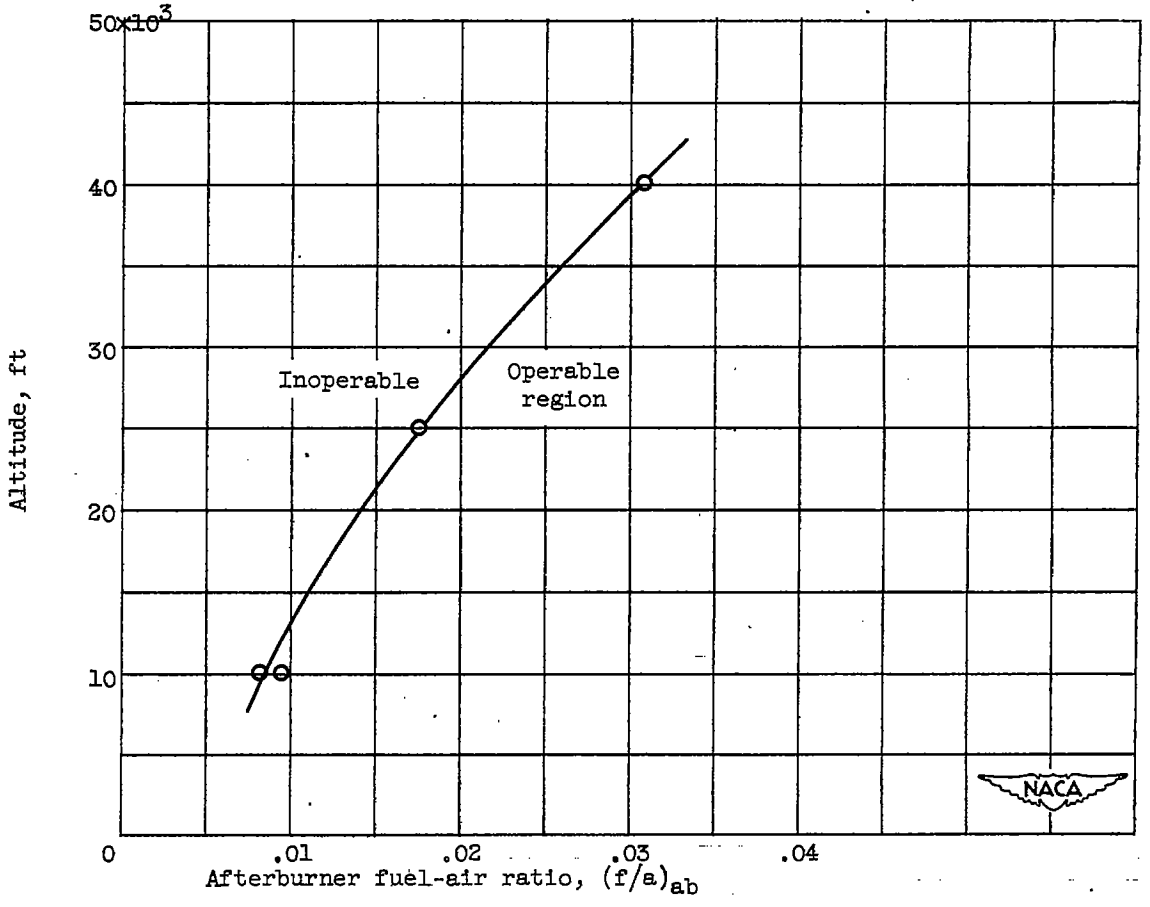

(b) Flight Mach number, 0.52.

Figure 11. - Effect of flight condition on afterburner lean blow-out.

[redacted]